Water Research 268 (2025) 122633

Contents lists available at ScienceDirect

Water Research

journal homepage: www.elsevier.com/locate/watres

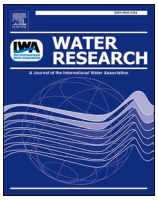

Riverine connectivity modulates elemental fluxes through a 200- year period of intensive anthropic change in the Magdalena River floodplains, Colombia

Jorge Salgado [a,b,c,*], Camila Jaramillo-Monroy [b], Andrés Link [d], Laura Lopera-Congote [e], Maria I. Velez [f], Catalina Gonzalez-Arango [d], Handong Yang [a], Virginia N. Panizzo [g], Suzanne McGowan [h]

[a] Department of Geography, University College London (UCL), Gower Street, London UK
[b] Programa de Ingeniería Civil, Universidad Católica de Colombia, Bogotá, Colombia
[c] Smithsonian Tropical Research Institute, Panama City, Republic of Panamá, Panamá
[d] Departamento de Ciencias Biológicas, Universidad de Los Andes, Bogotá, Colombia
[e] Department of Geology and Environmental Science, University of Pittsburgh, USA
[f] Department of Earth Sciences, University of Regina, Regina, SK, Canada
[g] School of Geography, University of Nottingham, Nottingham, UK
[h] Department of Aquatic Ecology, Netherlands Institute of Ecology (NIOO-KNAW), Wageningen, the Netherlands

ARTICLE INFO

Keywords:
Biogeochemistry
Climate variability
Floodplain lakes
Eutrophication
Magdalena River
River damming
Palaeolimnology
Sediment pollution
Tropical Rivers

ABSTRACT

Tropical floodplain lakes are increasingly impacted by human activities, yet their pathways of spatial and temporal degradation, particularly under varying hydrological connectivity regimes and climate change, remain poorly understood. This study examines surface-sediment samples and ^{210}Pb-dated sediment cores from six floodplain lakes, representing a gradient in hydrological connectivity in the lower Magdalena River Basin, Colombia. We analysed temporal and spatial variations in several sediment biogeochemical indicators: the concentration and flux of nutrients, heavy metals, and organic matter (OM), and redox conditions, flooding and erosion. Multiple factor analysis (MFA) of surface-sediments identified redox conditions, OM, flooding, heavy metals and lake connectivity as the main contributors to spatial variability within- and between-lakes sediments, accounting for 48 % of the total variation. Additionally, no clear distinction was found between littoral and open-water sediment characteristics. Isolated lakes sediments exhibited reductive conditions rich in OM and nutrients, whereas connected lakes sediments showed greater heavy metal enrichment and higher concentrations of coarse river-fed material. Generalised additive models identified significant changes in the biogeochemical indicators since the late 1800s, that accelerated post-1980s. Shifts in OM, erosion, flooding, redox conditions, land-cover change, heavy metals and climate were identified by MFA as the main drivers of change, explaining 60 %-71 % of the variation in the connected lakes and 53 %-72 % in the isolated lakes. Post-1980s, connected lakes transitioned from conditions of higher accumulation of OM and little erosion to higher accumulation of heavy metals and river-fed material. Conversely, isolated lakes, shifted from detrital-heavy metal-rich sediments to OM-, and nutrient-rich, reductive sediments. Sedimentation rates also surged post-1980s, particularly in highly connected lakes, from 0.14 ± 0.07 g cm^2 yr^{-1} to 0.5 ± 0.5 g cm^2 yr^{-1}, with elevated fluxes of metals, OM and nutrients. These changes in sediment biogeochemistry align with deforestation, river regulation and prolonged dry periods, highlighting the complexities behind establishing reliable reference conditions for pollution assessments in large, human-impacted tropical river systems.

* Corresponding author.
E-mail address: jorge.salgado@ucl.ac.uk (J. Salgado).

https://doi.org/10.1016/j.watres.2024.122633
Received 20 May 2024; Received in revised form 12 October 2024; Accepted 14 October 2024
Available online 15 October 2024

1. Introduction

Tropical floodplain lakes constitute unique ecosystems that serve as crucial connectors between aquatic and terrestrial habitats within a river basin (Nanson and Croke, 1992). These ecosystems offer invaluable services including the mitigation of peak flows during flood events, improving water quality, the bioprocessing, redistribution and sequestration of organic matter (OM), nutrients, sediments, and heavy metals (Wohl, 2021; Sutfin et al., 2016; Schindler et al., 2014).

The functioning of tropical floodplain lakes is primarily regulated by the interaction of regional precipitation and geomorphic conditions, which together influence the flow of rivers and the associated lateral exchange of materials (Junk et al., 1989). During high floods, nutrients, OM and key river-fed elements such as magnesium (Mg), titanium (Ti), iron (Fe) and aluminium (Al) are delivered into the lakes and are later returned to the main river as waters recede (Pereira et al., 2024; Junk et al., 1989). This deposition and remobilisation of elements across floodplains further depends on the degree of hydrological connectivity to the main river (Pestana et al., 2019; Almeida et al., 2014). For instance, isolated lakes, with lower degree of connectivity, receive marginal riverine input and rely more on local production, while highly connected lakes are more influenced by flooding events (Sutfin et al., 2016).

Unfortunately, the regional interplay of climate, geomorphology and hydrology renders floodplain lakes highly susceptible to current human pressures (Tockner and Stanford, 2002). The expansion of agriculture and urbanisation across river catchments are, for instance, a major driver of degradation (Rajib et al., 2023). Recent global assessments show that over the last three decades, approximately 600,000 km^2 of floodplain areas have been altered to meet growing socio-economic demands, where in tropical South America, about 80 % of floodplain changes are due to agriculture (Rajib et al., 2023). Additionally, river damming for hydropower, is leading to water quality degradation, reductions in river flow movement and magnitude, and alterations in the lateral movement of nutrients, OM, and river-fed elements into floodplain lakes (Wohl, 2021; Angarita et al., 2018; Winemiller et al., 2016).

In human-altered floodplains, floods still play a key role in transporting and depositing pollutants (Ciszewski and Grygar, 2016). During floods, concentrations of suspended particulate matter and pollutants surge and remain elevated as waters recede (Ciszewski and Grygar, 2016). Strong flood pulses bring an extra influx of dissolved OM and pollutants like arsenic (As), mercury (Hg), and lead (Pb), while particulate-bound pollutants such as zinc (Zn), nickel (Ni), and copper (Cu) tend to dilute and be present in lower concentrations (Monteiro et al., 2024; Almeida et al., 2014). Hydrological variations, influenced by redox changes in sediments, cause further pollutant levels to rise (decrease) during dry (wet) periods (Gaiero et al., 1997).

While flood-exposed lakes in human-impacted landscapes remain vulnerable to higher pollutant influxes, urban and industrial sources are increasingly becoming the primary drivers of lake pollution (Luo et al., 2021; Ciazela et al., 2018). As a result, proximity to a point source is often a more significant factor than flood pulses alone. Such increasing role of anthropic point sources highlights the need for long-term records to establish baseline conditions and characterise river pulse-pollutant dynamics over decades to centuries. Recent studies suggest that lake sediments serve as reliable archives of the history of human impact, past floods, and changes in connectivity (Walton et al., 2023; Lopera-Congote et al. 2021; Salgado et al., 2019b). Variations in OM and grain size are used for instance, as proxies to infer flow energy and connectivity: high OM accumulation, fine-grained silts and clays reflect moderate flows, while low OM content and coarse-grained sediments indicate high-energy flood events (Schillereff et al., 2014). To date, most palaeoflood research has focused on millennial-scale records to assess climatic drivers and/or specific events (Schillereff et al., 2014). Its potential to track hydrological shifts and human pollution on decadal-century scales in tropical regions lacking long-term instrumental data remains, however, underexplored.

The lower Magdalena River Basin (LMRB) in Colombia (Fig. 1), exemplifies a critically endangered floodplain ecosystem, heavily influenced by human activity (Jiménez-Segura et al., 2022; Salgado et al., 2022). Spanning approximately 320,000 hectares of natural floodplains and lakes (locally known as *Ciénagas*), it is one of the largest, lowland, tropical floodplains in South America. Located within the Tumbes–Choco biodiversity hotspot (Myers et al., 2000), the LMRB is ecologically vital, hosting over 160 aquatic vertebrate species and two protected sites under the Ramsar convention (Wittmann et al., 2015): *Complejo Cenagoso de Zapatosa* (121,725 ha) and *Ciénaga Grande de Santa Marta* (400,000 ha). Home to over 6 million people, the LMRB is also one of the most densely populated floodplains in tropical America, making it highly vulnerable to human pressures such as river damming for hydropower, land-cover changes for agriculture and urbanisation, the invasion of alien species and the impacts of climate change (Munar et al., 2023; Salgado et al., 2022; Angarita et al. 2018).

Extensive agriculture, combined with atmospheric deposition and industrial and household sources of pollution, has led to excessive loads of nutrients, heavy metals and OM into the LMRB (Yang et al., 2023; Tejeda-Benitez et al., 2016). For instance, the biogeochemical cycles of nitrogen (N) and phosphorus (P) have been significantly disrupted, with current concentrations in the main river now exceeding pre-1950 levels by one order of magnitude (Jiménez-Segura et al., 2022). Similarly, toxic metals levels such as Pb, Hg, and As have increased throughout the river system, with bioaccumulation in aquatic life and humans, reaching levels three times higher than WHO recommendations (Córdoba-Tovar et al., 2022; Olivero-Verbel et al., 2015a).

Here, we integrate palaeolimnological techniques from six lakes in the Barbacoas-Chucurí floodplain lake network (Fig. 1) and contemporary and historical precipitation and land-use records in the LMRB. By analysing long-term (years to centuries) changes in sedimentation rates, OM content, heavy metals, redox conditions, flooding patterns and nutrient levels, from ^{210}Pb-dated lake sediment cores, we aim to assess the pathways through which ecosystem degradation occurs. We also aim to quantify how climate variability and the degree of connectivity modulate these responses and understand how ecosystems respond over time to river damming, flooding, deforestation and proximity to pollution sources.

2. Methods

2.1. Study area

The Barbacoas-Chucurí floodplain lake network is situated in the middle, lowland (< 90 m.a.s.l) stretch of the LMRB (Fig. 1). This lake network primarily receives inflow from the Magdalena River (mean discharge= 7100 m^3 s^{-1}) and its tributary, the Carare River (mean discharge= 508 m^3 s^{-1}). Additionally, a smaller creek, The San Juan, which originates from the eastern flank of the Eastern Andean Cordillera, contributes to the Carare River.

The region experiences a bimodal precipitation pattern, with two main rainy seasons (March-May and October-November) and two dry seasons (December-February and June-September). Variations in precipitation are controlled by El Niño-Southern Oscillation (ENSO), which occurs every 2–5 years. In this region, the El Niño warm phase of ENSO, leads to intense and prolonged droughts, significantly reducing river-lake connectivity (Jiménez-Segura et al., 2022). In contrast, during the cold phase of ENSO or La Niña, the region receives ca. 30 % more rain than in normal years, causing widespread flooding, and increasing river-lake connectivity (Jiménez-Segura et al., 2022).

2.1.1. Study lakes

Six floodplain shallow (mean depth = 2.3 ± 0.8 m) lakes were studied: San Juana (surface area: ~105 ha), Colorada (~43 ha), Rabona (~114 ha), Chucurí– Aguas Blancas (AB, ~125 ha), Chucurí– Aguas

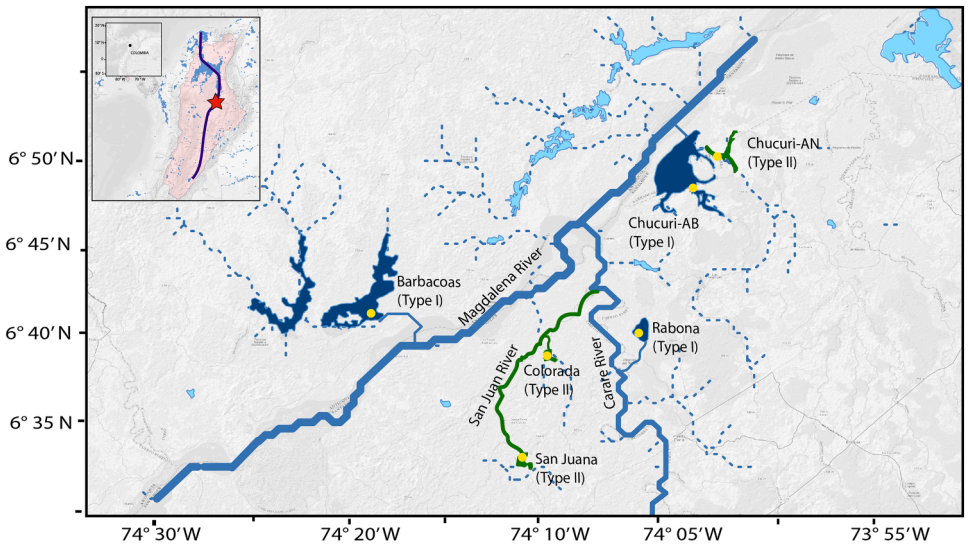

Fig. 1. Location of the Barbacoas-Chucurí lake network within the lower Magdalena River basin (marked by the red star) and the position of the six study lakes, along with the coring sites at each lake (indicated by yellow circles). The lakes are classified based on their hydrological connectivity to a main river: *Type I* lakes (shown in dark blue), which are directly connected through a channel (Barbacoas, Chucurí -AB, and Rabona); *Type II* lakes (shown in green), which are connected through a secondary channel (San Juana and Colorada) or another lake (Chucurí-AN).

Negras (AN, ~114 ha), and Barbacoas (~100 ha) (Fig. 1). These lakes receive large amounts of humic compounds from nearby wetlands and remnants of riparian forest (Moreno et al., 1987; Pedraza et al., 1989), resulting in low water transparency (mean Secchi depth = 0.8 ± 0.2 m), low dissolved oxygen (DO; mean= 3.5 ± 1.5 mg L^{-1}) and circumneutral pH (mean= 7.3 ± 0.3) (Table 1). Lake levels fluctuate significantly (±2.5 m; personal observation) between rainy and dry seasons, with littoral and open water areas often desiccating late in the dry season. During dry El Niño periods, the lakes can lose 30–70 % of their open water surface area (Lopera-Congote et al., 2021).

The lakes are situated within cattle ranches, and oil palm plantations, with only small remnants of riparian forest. The region experienced significant deforestation, with nearly 10,000 hectares yr^{-1} being lost between 2005 and 2010 (Jiménez-Segura et al., 2022). Small towns (~500 inhabitants) are present at the mouths of the Carare and Magdalena rivers and the area also faces oil exploitation and small-scale open-cast gold and gravel mining operations.

2.1.2. River-lake connectivity

The lakes were classified into two types based on their hydrological connection to the Magdalena and Carare Rivers, following Jiménez-Segura et al., 2022 (Fig. 1): *Type I* includes lakes directly

Table 1
Average (Avg.) values and standard deviations (SD) categorised by lake sampling points of water chemistry parameters at littoral (L) and open water (OW) are as.

Lake		Lake type	Area	Depth (m)	DO (ppm)	T (°C)	Secchi depth (m)	pH
Barbacoas	*Avg.SD*	I	L	2.3 ± 0.9	2.7 ± 1.7	31.6 ±1.3	0.8 ±0.1	7.5 ± 0.3
Chucurí-AB	*Avg. SD*	I	L	2.2 ± 0.1	4.8 ± 0.1	32.7 ± 0.7	0.8 ±0.5	7.2 ± 0.2
Rabona	*Avg. SD*	I	L	1.3 ± 0.2	2.5 ± 0.8	31.3 ± 2.6	1.0 ±0.1	7.7 ±0.1
Chucurí-AN	*Avg. SD*	II	L	2.2 ± 0.1	4.8 ± 0.1	33.2 ± 0.1	1.1 ±0.02	7.8 ± 0.3
Colorada	*Avg. SD*	II	L	1.1 ± 0.5	3.6 ± 0.1	29.8 ± 0.1	0.7 ±0.1	7.5 ± 0.1
San Juana	*Avg. SD*	II	L	2.2 ± 0.1	1.2 ±0	31.2 ±0.6	0.6 ±0	7.7 ± 0.3
All	**Avg.**		**L**	**1.8**	**3.3**	**31.6**	**0.8**	**7.6**
	SD			**0.5**	**1.4**	**1.2**	**0.2**	**0.2**
Barbacoas	*Avg. SD*	I	OW	2.5 ± 0.3	3.1 ± 1.1	30.1 ± 0.3	0.7 ±0.2	7.3 ± 0.3
Chucurí-AB	*Avg. SD*	I	OW	3.4 ± 0.5	5.4 ± 0.4	32.9 ±1.1	1.0 ±0.4	6.8 ±0.2
Rabona	*Avg. SD*	I	OW	2.1 ± 0.2	2.7 ± 0.1	31.1 ± 0.5	1.0 ±0	7.2 ± 0.1
Chucurí-AN	*Avg. SD*	II	OW	3.9 ± 0.1	5.2 ± 0.05	32.3 ± 0.1	1.2 ±0.1	7.4 ±0
Colorada	*Avg. SD*	II	OW	1.6 ±0	4.1 ± 0.2	29.7 ±0	0.7 ±0.1	7.1 ± 0.1
San Juana	*Avg. SD*	II	OW	2.9 ± 0.1	0.9 ± 0.7	31.3 ± 1.6	0.7 ±0.1	7.3 ± 0.1
All OW	**Avg.**		**OW**	**2.7**	**3.6**	**31.2**	**0.9**	**7.2**
	SD			**0.8**	**1.7**	**1.2**	**0.2**	**0.2**

connected to a main river, such as Barbacoas and Chucurí-AB (connected to the Magdalena) and Rabona (connected to the Carare). *Type II* comprises more isolated lakes connected through secondary waterbodies, like San Juana and Colorada (via San Juan creek to the Carare) and Chucurí-AN (connected to the Magdalena through Chucurí-AB). Despite being part of the same system, Chucurí-AB and Chucurí-AN were treated separately due to differences in watercolour, size, and connectivity.

2.2. Water physicochemistry and surface sediment sampling

A fieldwork campaign was conducted in August 2022 to collect multiple surface-sediment samples (top 2 cm) at each lake from both littoral and open water habitats. The samples were retrieved using a short, wide-bore corer with a diameter of 10 cm (Aquatic Instruments Inc.) aimed to assess spatial variability in the fossil record. For each of the smaller lakes - San Juana, Colorada, Rabona, and Chucurí-AN - two samples in both open water and littoral habitats were collected. For the larger lakes - Chucurí-AB and Barbacoas - three samples in open water and littoral habitats were collected in each lake. Sediments were stored at 4 °C prior to analyses. Water temperature (°C), pH, DO (mg L^{-1}), Secchi depth (m), and water depth (m) were also measured at each surface sediment sampling location using a YSI probe.

2.3. Core sampling

Sediment coring was conducted in June 2017. Single, short cores of approximately 50 cm long were collected using a wide-bore corer in the following lakes: Colorada (core code: LCOL1), Rabona (LRAB1), Chucurí-AB (LCHUC-AB1), and Chucurí-AN (LCHUC-AN1). The specific coring locations and water depth were: 90 cm for LCOL1 (6°42′20.80″N 74° 8′16.50″W), 105 cm for LCHUC-AB1 (6°48′32.40″N 74° 2′13.48″W), 135 cm for LCHUC-AN1 (6°50′4.47″N 74° 2′5.67″W), and 95 cm for LRAB1 (6°42′53.01″N 74° 4′39.89″W), respectively (Fig. 1). Two additional cores, previously collected and studied from San Juana Lake (LSAN1) and Barbacoas Lake (LBARB1) in 2016 by Lopera-Congote et al. (2021) were also included in this study. These cores were collected using the same methods as in 2017, from water depths of 100 cm (6°38′32″N 74°09′24″W) for LSAN1 and 90 cm (6°44′26″N 74°14′36″W) for LBARB1 cores. Cores were taken from secluded bays where wind patterns favoured sediment transport and deposition and where a mix of littoral wetland fringes and open waters, allows assessing potential temporal shifts in OM sources between littoral and open water. In the field, all cores were extruded at 1-cm intervals and refrigerated at 4 °C for further analysis.

2.4. Dating and age-depth models

The cores LSAN1, LBARB1, LCOL1 and LCHUC-AB1 were dated using radiometric measurements of ^{210}Pb, ^{226}Ra, ^{137}Cs, and ^{241}Am by direct gamma assay (Appleby, 2001) in the Environmental Radiometric Facility at University College London, UK. Age models for LSAN1 and LBARB1 cores were derived from Lopera-Congote et al. (2021). For LCOL1 and LCHUC-AB1, the top 20 cm of the cores were dated, and chronologies were calculated using the constant rate of ^{210}Pb supply (CRS) dating model (Appleby, 2001). An age model beyond the top 20 cm for all four cores was fitted, by simulating new ages following a shape-constrained generalised additive model (GAM), with the age-model spline constrained by a monotonic decline (Simpson, 2018). The ^{210}Pb Chronologies for cores LRAB1 and LCHUC-AN1 were established by correlation with OM profiles of cores LCOL1, LSAN1 and LCHUC-AB1 following Salgado et al. (2019a) (Appendix 2: Fig. S2).

2.5. Geochemical analysis

Concentrations (μg/g) of geochemical elements in the LSAN1 and LBARB1 cores were measured using an Xmet 7500 portable X-ray fluorescence (XRF) analyser (Oxford Instruments Inc.) (Lopera-Congote et al., 2021). Three grams of dry sediment per 1-cm-thick sample were analysed, with a 1-cm sampling resolution for the top 18 cm and every 3 cm for the remaining depths in both cores. For the LCOL1, LRAB1, LCHUC-AB1, and LCHUC-AN1 cores, element concentrations were analysed using a PANalytical Epsilon3-XL XRF spectrometer (Malvern Panalytical Inc.) at the School of Geography, University of Nottingham, UK. Each 1-cm-thick sample was analysed with a 2-cm sampling resolution. Both XRF methods were calibrated against certified reference materials prior to analysis.

Specific elements and ratios were used as proxies for redox conditions, flooding, erosion and pollution (nutrients and heavy metals). For heavy metals we use Ni, Cu, Zn, As, Pb, chromium (Cr), cobalt (Co), and cadmium (Cd), and for nutrients we use P and N. Erosion (detrital inputs), and flooding were assessed using specific element ratios of titanium–calcium (Ti/Ca), and zirconium–iron (Zr/Fe), respectively (Davies et al., 2015). Ti is a redox-insensitive element and an unambiguous indicator of catchment erosional inputs, while Ca may reflect in-lake carbonate production (Davies et al., 2015). Thus, higher Ti/Ca ratios provide information about detrital erosion from runoff (Salgado et al., 2020). During high floods, coarse-grained (Zr) sediments often increase over finer Fe-rich sediments, hence, higher Zr/Fe ratios can be used to indicate flood events (Schillereff et al., 2014).

Reductive conditions were assessed using the iron-manganese (Fe/Mn) ratio (Davies et al. 2015) and increases in molybdenum (Mo), vanadium (V) and sulphur (S) (Zhang et al., 2022; Tribovillard et al., 2006). In reducing sediments, Fe and Mn solubility increases, with Mn being more sensitive to these changes, thus, higher Fe/Mn ratios can indicate anaerobic conditions (Davies et al., 2015). Anoxic conditions in lake sediments can also lead to sulphur incorporation (Tribovillard et al., 2006). Anoxic environments are enriched in redox-sensitive elements like Mo and V s due to reactions with sulphide, leading to higher concentrations relative to conservative elements like Al or Ti (Tribovillard et al., 2006). Due to a lack of Al data availability across the 6 cores and robust background levels of Mo and V in the study area, we calculated Mo and V enrichments by normalising them to Ti (Tribovillard et al., 2006).

The OM in the surface and core sediments were measured by loss-on-ignition (LOI) at 550 °C (Dean, 1974). Core sampling resolution was at every 2 cm for the top 20 cm samples and at every 4 cm for the remaining 30 cm of the core's samples. The sources (allochthonous versus autochthonous) of OM were then determined using the ratios of total percentage organic carbon (TOC) and total organic nitrogen (TN), obtained by combustion of dry sedimentary material on a Costech Elemental Analyzer (EA) coupled in-line to a dual-entry VG TripleTrap and Optim mass spectrometer at the National Environmental Isotope Facility, British Geological Survey, UK.

We then used the mass accumulation rates (MAR; expressed as gr cm^{-2} yr^{-1}) obtained from the ^{210}Pb dating models to determine the flux of OM, nutrients and metals. Fluxes were calculated by multiplying the MAR, the LOI percentage or elemental concentrations and the dry bulk density. Thus, metal, OM and nutrient fluxes were derived only from the ^{210}Pb dated cores LCHUC-AB1 and LBARB1 (*Type I*) and LSAN1 and LCOL1 (*Type II*), focusing on the dated period from approximately 1950 to the present.

2.6. Historical climate

Long-term climatic variability data (1950-present) were obtained from the Standardised Precipitation-Evapotranspiration Index (SPEI) analysis (Vicente-Serrano et al., 2010). The SPEI analysis generates a drought index based on the difference between precipitation and potential evapotranspiration for a given area, allowing the identification of years with extreme water deficit or excess.

2.7. Historical Land-cover

Historical land cover changes in Colombia were estimated using the Hyde 3.2 database (Klein Goldewijk et al., 2017), which provides annual data from 2000 onwards and decadal data prior to 2000. This dataset assesses historical population, pastureland (meadows and grasslands in Mkm^2) and irrigation areas (in 1000 ha), integrating satellite data to produce spatially explicit maps at a 5-arcmin resolution from 10,000 BCE to the present. Although these data are at national scale, they likely capture key historical changes in the LMRB, given the fact that much of Colombia's socio-economic development has historically occurred within this river basin.

2.8. Baselines and degree of pollution

To contextualise our findings within the broader LMRB framework, we used secondary data from the Magdalena River's middle stretches (Tejeda-Benitez et al., 2016) and two comparable lakes, Opon and Miramar, located south of our study area (Olivero-Verbel et al., 2015b). Both Opon and Miramar lakes are directly connected to the Magdalena River (*Type I*) and have experienced significant anthropogenic impacts, with Miramar now classified as an urban lake within the city of Barrancabermeja (Olivero-Verbel et al., 2015b). These sedimentological reference data were used to compare pre-industrial sediment core levels with current elemental concentrations in the studied lakes.

2.9. Data analysis

2.9.1. Gradients of geochemical, climatic and land-use change

Spatial and temporal gradients in sediment biogeochemistry, water physicochemistry, climatic, and land-cover changes in the lakes were assessed using Multiple Factor Analysis (MFA) (Pagès, 2002). MFA simultaneously evaluates categorical variables (e.g., lake locations and connectivity types) and continuous variables, including redox proxies (Fe/Mn, Mo/Ti, S/Ti, V/Ti), erosion (Ti/Ca), flooding (Zr/Fe), nutrients (P, N), heavy metals (Mn, Cr, Co, Ni, Cu, Zn, As, Cd, Pb), OM (LOI, C/N), water physicochemistry (DO, pH, temperature, depth), land-cover changes (pastureland, irrigation), and climate (SPEI). Continuous data were standardised to reduce skewness and ensure comparability (Pagès, 2002). MFA was performed in R using the FactoMineR package (Le et al., 2008), and missing values were addressed with imputation techniques from the "missMDA" package.

2.9.2. Significant periods of temporal change

Generalised additive models (GAMs) from the "mgcv" package in R (Wood, 2017) were used to identify significant temporal trends in the sediment biogeochemical indicators, climatic and land-cover datasets with smooth functions (Simpson, 2018). For each lake, principal curve (PrC) analysis (R "analogue" package; Simpson, 2007) derived a main gradient of variation in the targeted biogeochemical indicators, which was then fitted in independent GAMs against time using smooth functions. The residual maximum-likelihood (REML) method and a Gaussian distribution with an identity link were used to model time series data, with a base function (k) of 10 for all lake data. Diagnostic Q-Q plots checked for residual variance homogeneity and addressed uneven observations. Significant compositional thresholds were assessed using the first derivative function of each GAM (R "gratia" package; Simpson, 2022), with deviations from 0 indicating periods of significant change (Simpson, 2018).

2.9.3. Single effects of land-cover change and climate variation

The unique effects of land-cover change (pastures and irrigation) and climatic variation (SPEI) on each lake's long-term sediment biogeochemical variation were analysed using partial redundancy analyses (pRDA; varpart function in the 'vegan' R package; Oksanen et al., 2022). Each component's contribution was adjusted to R^2. pRDA decomposed the total variance into four parts: (a) land-cover, (b) climate, (c) shared, and (d) unexplained variation. The shared fraction (c) indicates variance attributed to both land-use and climatic factors. The significance of each component was assessed through 499 Monte Carlo permutations.

2.9.4. Changes in elemental fluxes and baseline conditions

Differences in biogeochemical parameters among lake surface-sediments, baseline palaeodata, and regional references were analysed using Tukey's Honest Significant Difference test ($p < 0.05$). To link erosional processes with land-cover changes, flux data were divided into three historical periods: 1950–1979, 1980–1997, and 1998-present. Mean values between these periods were also compared using Tukey's HSD test ($p < 0.05$).

3. Results

3.1. Age models

The ^{210}Pb age models are provided in Appendix 1. To summarise, LSAN1, LCOL1, LCHUC-AB1 and LBARB1 cores indicate that the last 100 years are contained approximately within the top 20–30 cm of the cores. The final age model for the more connected *Type I* lakes (LBARB1, LCHUC-AB1), spanned to 1959 CE in LBARB1, to 1950 CE for LCHUC-AB1 and to 1910 CE for LRAB1 (Appendix 1: Figure S1.1). In contrast, for the more isolated *Type II* lakes, the models suggest a sediment record spanning to approximately 1620s CE in LSAN1, 1750s CE in LCOL1 and 1910 CE for LCHUC-AN1 cores.

3.2. Spatial gradients in lake biogeochemistry and limnology

The first two dimensions of the MFA on the surface-sediments accounted for 48 % (Dimension 1: 32 %; Dimension 2: 1 6 %) of the biogeochemical indicators and water chemistry variables variation (Fig. 2). Dimension 1 separated the data into two groups: lakes located in the south of the area (Barbacoas and San Juana) and those located in the north (Colorada, Rabona, and both Chucuri lakes). Dimension 2 differentiated lake connectivity types, with the highly connected *Type I* lakes (Barbacoas, Chucuri- AB, and Rabona) situated on the positive side of dimension 2, and the more isolated *Type II* lakes (Chucuri-AN, San Juana and Colorada) on the negative side of dimension 2.

For Dimension 1, key contributors were redox conditions (16 %), OM (LOI and C/N; 15 %), lake categories (14 %), flooding (Zr/Fe; 13 %), and heavy metals (11 %). For Dimension 2, notable contributions came from lake categories (34 %), connectivity type (30 %) and redox conditions (12 %) (Appendix 2: Fig S2.1). The analysis identified two types of lake sediment biogeochemistry: one with high OM and elevated TP and TN levels, and another high in inorganic, heavy metal concentrations and signs of increased erosion, flooding and reductive conditions. Some spatial biogeochemical variations were observed within lakes, but with no clear distinctions between littoral and open waters.

3.3. Long-term gradients in sediment biogeochemistry, land-cover and climate

The full stratigraphic lake plots for the analyses of each core data are presented in Fig. 3 and the main temporal compositional changes revealed from the GAMs and MFA (Figs. 3, 4) analyses are summarised below:

3.3.1. Periods of significant temporal change

The GAMs revealed a gradual shift in the sediment geochemical patterns across lakes since the late 1800s, with a notable period of acceleration around the mid 1980s that stabilised thereafter (Fig. 5i, ii). Although there was a consistent temporal and regional trend of change in the lake sediments, the MFA indicated a distinct spatial response between the lakes according to the river-lake connectivity types (see

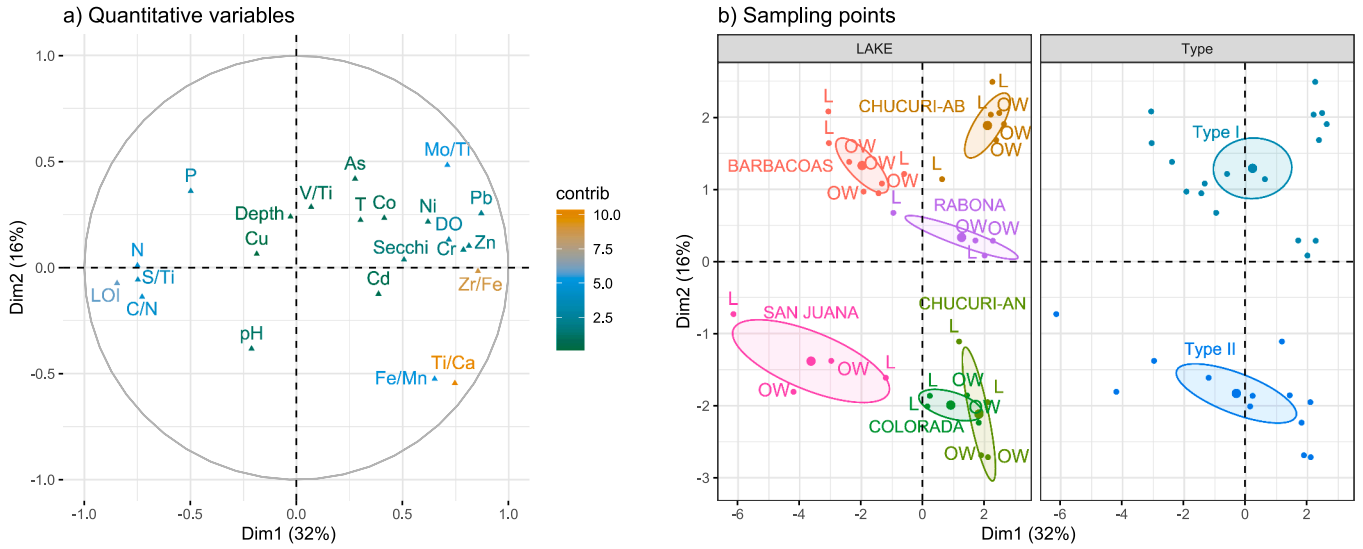

Fig. 2. Multiple Factor Analysis (MFA) plots illustrating: (a) the variations of OM (LOI and C/N), redox conditions (Fe/Mn, S/Ti, V/Ti and Mo/Ti), flooding (Zr/Fe ratio), erosion (Ti/Ca ratio), heavy metals (Mn, Cr, Co, Ni, Cu, Zn, As, Cd, and Pb), nutrients (P and N), and water chemical parameters (DO, surface temperature [T], pH, Secchi depth, and water depth) in the surface-sediments of the lakes. The pale brown background represents conditions high in OM, while the blue background indicates environments dominated by heavy metals, erosion, flooding, and reductive conditions; (b) The sampling locations within each lake are categorised by hydrological connectivity type: *L* = littoral; OW= open water.

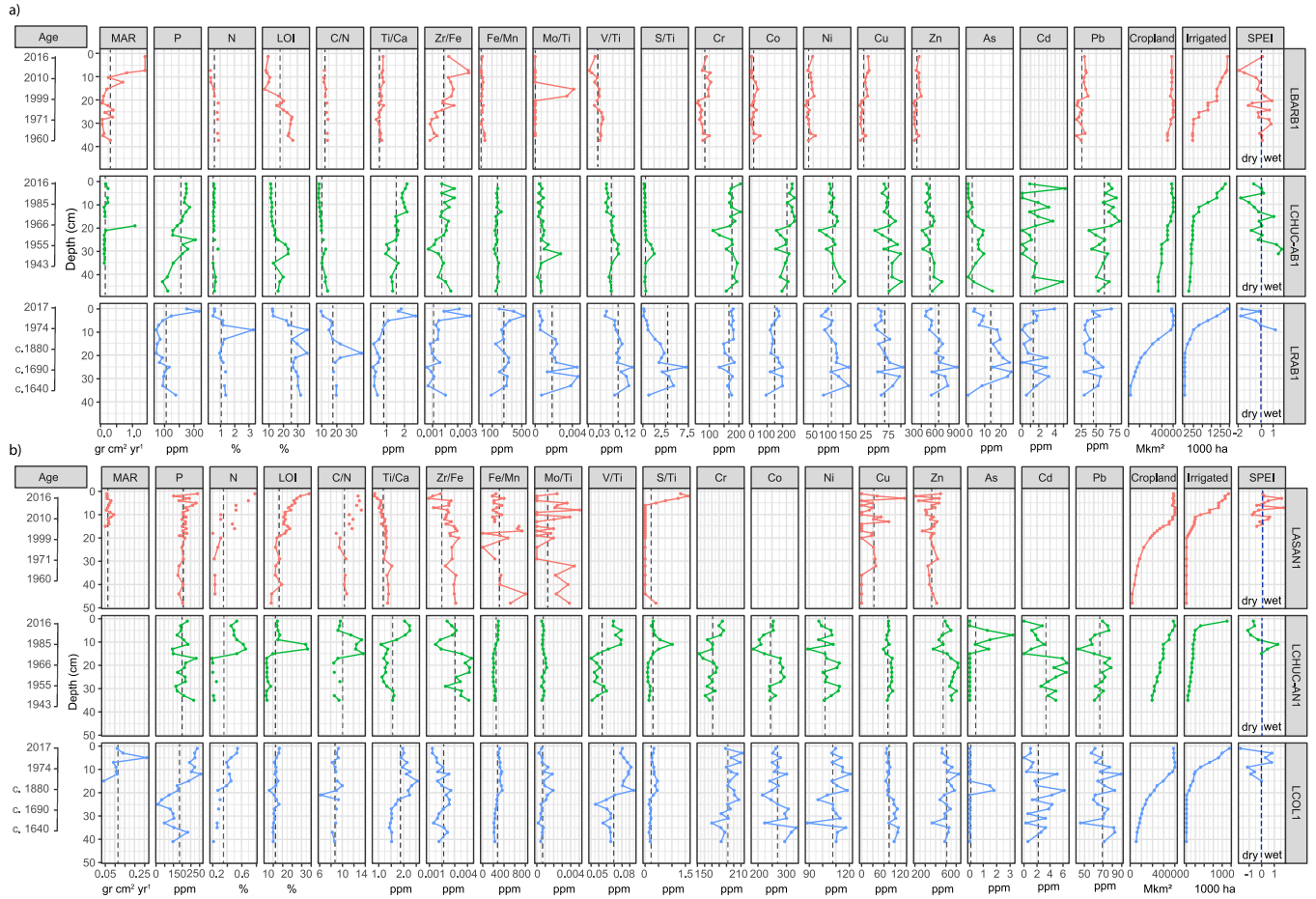

Fig. 3. Stratigraphic plot showing the long-term variation in biogeochemical elemental concentrations and mean values (dash vertical lines) in (a) connected lakes (*Type I*); and (b) more isolated lakes (*Type II*). Wet and dry interannual periods as indicated by SPEI are also shown by a blue vertical line.

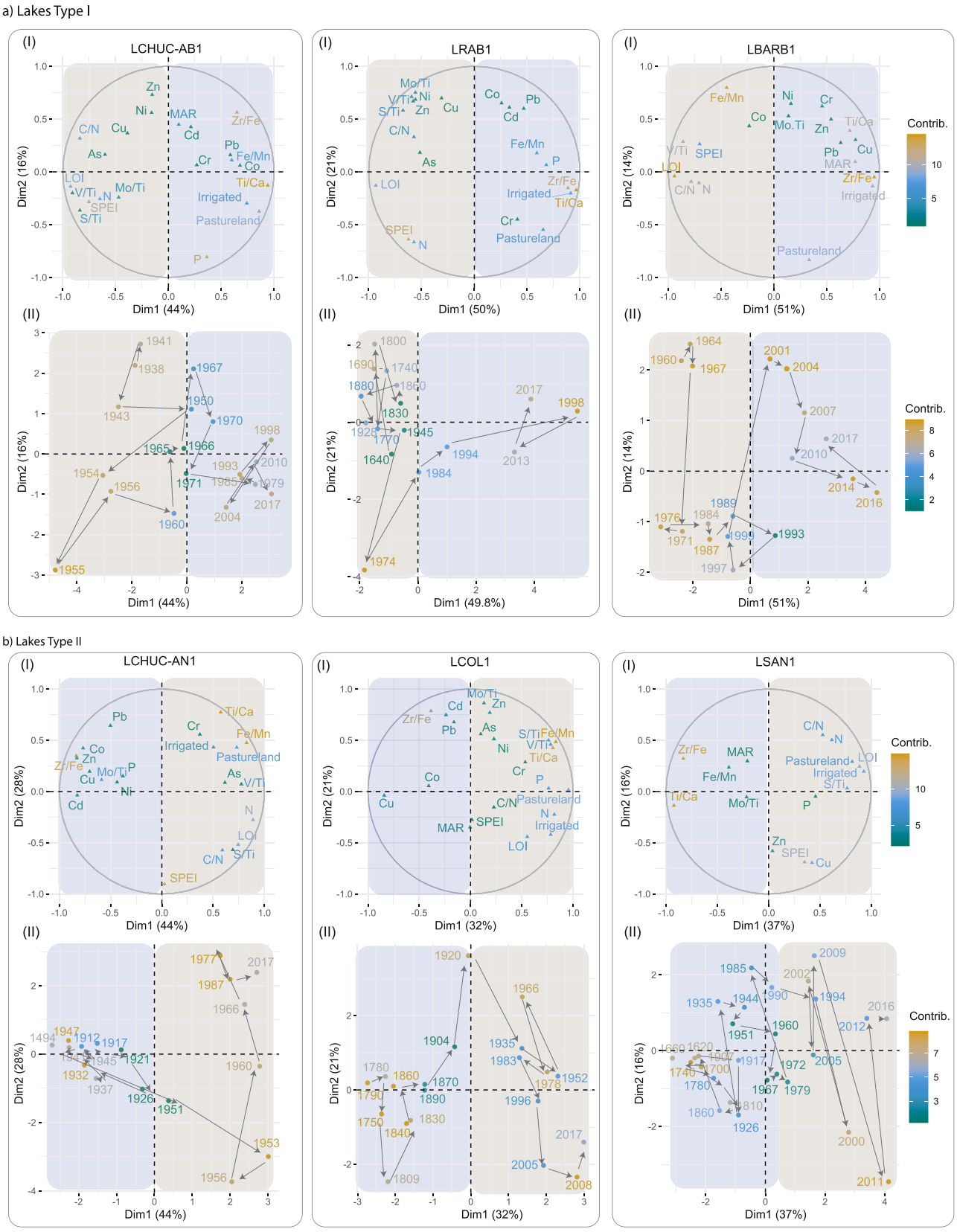

Fig. 4. MFA plots depicting the temporal variation (I) of OM (LOI and C/N), flooding (Zr/Fe ratio), erosion (Ti/Ca ratio), redox conditions (Fe/Mn, S/Ti, V/Ti, and Mo/Ti ratios), heavy metals (Mn, Cr, Co, Ni, Cu, Zn, As, Cd, and Pb), nutrients (P and N), land-cover change (cropland and irrigated land) and the trajectory of temporal change (II) in the multivariate space in sediment cores from (a) *Type I* lakes (LCHUC-AB1; LRAB1; LBARB1) and (b) *Type II* lakes (LCHUC-AN1; LCOL1; LSAN1). The pale brown background indicates conditions rich in OM, while the blue background signifies conditions rich in heavy metals, erosion, flooding, and redox conditions.

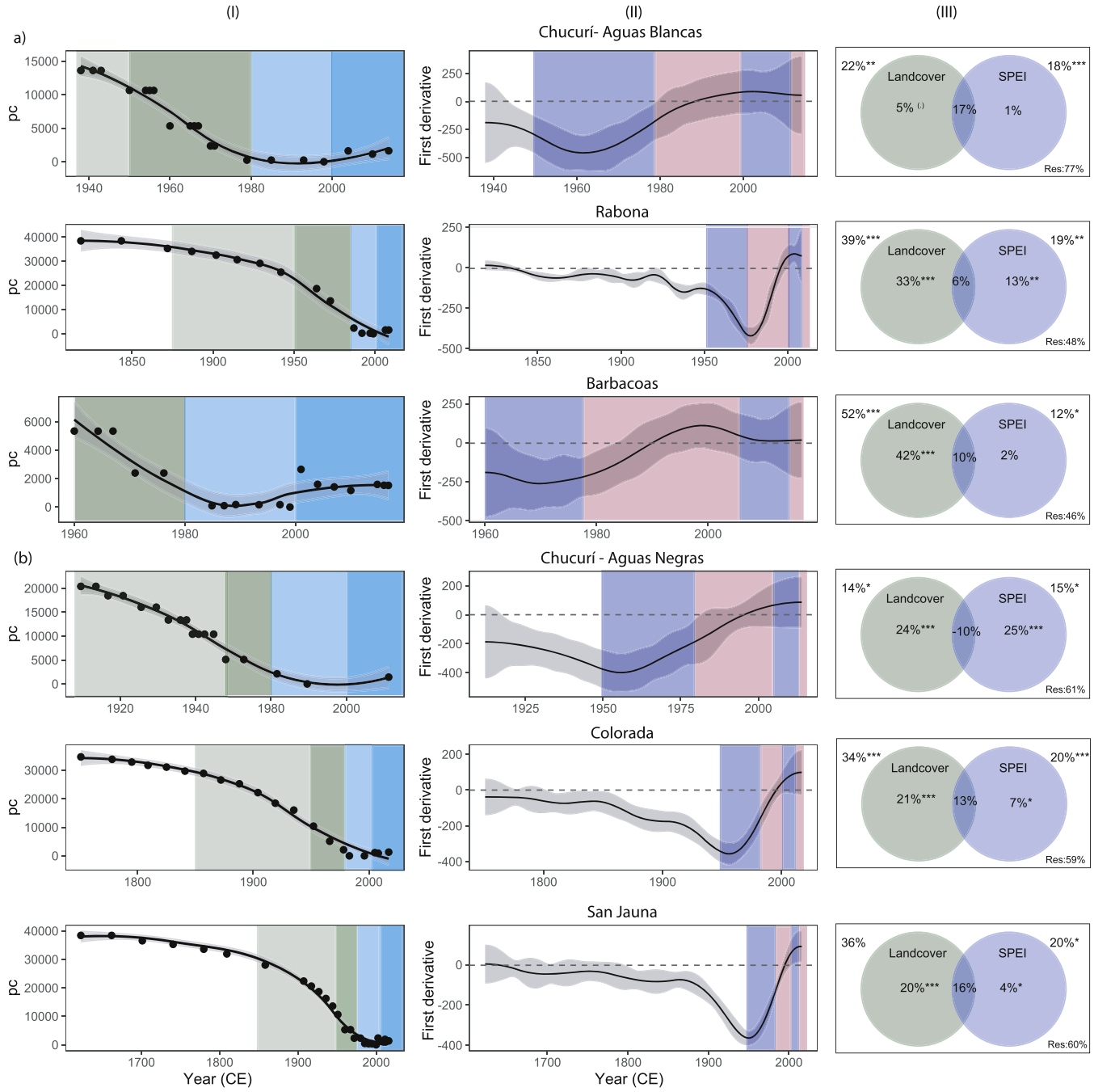

Fig. 5. Generalised additive model (GAM) plots of long-term biogeochemical change derived from a principal curve analysis (PC) found in the sediment cores of lakes *Type I* (a) and *Type II* (b). (i) Changes in PC scores over time. The onset of deforestation (mid 1800s-1950) and subsequent periods of increased deforestation (1950–1979; 1980–1997; 1998-present CE) are represented by a background colour from pale green to pale blue. (II) significant periods of change determined by each GAM model first derivate. First derivative values deviating from the 0 (dash line) indicate a significant period of change. Intervals related to SPEI extreme dry conditions (ENSO-El Niño) are indicated by a red background and extreme wet (ENSO-La Niña) phases in blue; and (III) pRDA results indicating the unique contribution of land-cover change and climate (SPEI) in the lakes long-term biogeochemical variation. * $p < 0.05$; ** $p < 0.01$; *** $p < 0.001$.

Fig. 4).

3.3.2. *Type I lakes*

The first two dimensions from the MFAs on cores LCHUC-AB1, LRAB1, and LBARB1 explained 60 %, 71 %, and 68 % of the total historical sedimentological variation, respectively (Fig. 4a). Dimension 1 accounted for 44–52 % of the variation, with significant contributions from OM, erosion, flooding, redox conditions, land-cover changes and SPEI (Appendix 3: Fig. S3.1a). Dimension 2 explained the remaining 16–21 % of the variation, with significant contributions of metals, flooding, redox conditions and SPEI.

The MFAs revealed that before the 1980s, the lakes sediments (on the negative side of Dimension 1) were characterised by reductive conditions (V/Ti and S/Ti) and high accumulation of OM (LOI and C/N), and of TN, As, Cu, and Ni. The associated SPEI values indicate wetter conditions. Post-1980s, sediment characteristics (on the positive side of Dimension 1) shifted to an inorganic phase with increased pastureland and irrigation, higher flooding, erosion, and reductive conditions (Fe/Mn and Mo/Ti) and higher concentrations of Cr, Cd, Co, and Pb.

3.3.3. Type II lakes

The first dimensions from the MFA on cores LCHUC-AN1, LCOL1, and LSAN1 explained 72 %, 53 %, and 53 % of the historical sedimentological, land-cover and climatic variation, respectively (Fig. 4b). Dimension 1 accounted for 32–44 % of the temporal variation in the lake's sediments, with significant contributions from OM, erosion, land-cover change, flooding and redox conditions (Fig. S3.1b). Dimension 2 explained 16–28 % of the variation, with heavy metals, SPEI and redox conditions significantly contributing the most (Fig. S3.1b).

The MFAs showed that pre-1950s, inorganic conditions prevailed in the lakes sediments (negative side of dimension 1) with prevalent flooding and higher levels of MAR, Cr, Cd, Co and Pb. Post-1950s, conditions shifted to high accumulation of OM, N, P and As, increased erosion and reductive conditions (S/Ti, V/Ti, Fe/Mn); all these under expanding pasturelands and irrigation (positive side of dimension 1).

3.4. Unique contributions of land-cover and climate

The pRDAs for *Type I* (connected lakes) revealed that land-cover changes explained 22 %, 39 %, and 52 % of the sediment biogeochemical variance in Chucurí-AB, Rabona, and Barbacoas lakes, respectively ($p < 0.05$) (Fig. 5a.iii). Climate factors (SPEI) accounted for 18 %, 19 %, and 12 % of the variance, respectively ($p < 0.05$). Adjusting for shared effects, land-cover change alone explained 5 % ($p = 0.9$) in Chucurí-AB and a significant ($p < 0.05$) 33 % and 42 % in Rabona and Barbacoas ($p < 0.05$). Climate alone explained an additional significant ($p < 0.05$) 13 % of the variance in Rabona Lake. The remaining variance (77 %, 48 %, and 46 %) was unexplained by land-cover change or climate.

The pRDAs for *Type II* (isolated lakes) showed that land-cover change significantly explained 14 %, 34 %, and 36 % of the biogeochemical variation in Chucurí-AN, Colorada, and San Juana lakes, respectively ($p < 0.05$) (Fig. 5b.iii). Climate factors accounted for 15 %, 20 %, and 20 % of the variance, respectively ($p < 0.05$). After adjusting for shared effects, land-cover change alone explained 24 %, 21 %, and 20 % of the variance ($p < 0.05$), while climate alone accounted for 25 %, 7 %, and 4 % ($p < 0.05$). The remaining variance (61 %, 59 %, and 60 %, respectively) was unexplained by both factors.

3.5. MAR and element fluxes (1950-present)

Aside from a notable increase in sedimentation in LCHUC-AB1 during 1955, *Type I* lakes saw a significant rise in mean MAR from 0.14 ± 0.07 g cm^2 yr^{-1} (1950–1979) to 0.5 ± 0.5 g cm^2 yr^{-1} (1998-present) ($p < 0.05$) (Fig. 6a). Similarly, fluxes of P (30.1 ± 8.2 to 51.0 ± 10.1 g cm^2 yr^{-1}), Cr (18.4 ± 10.0 to 50.3 ± 40.7 g cm^2 yr^{-1}), Ni (11.3 ± 7.0 to 24.4 ± 19.2 g cm^2 yr^{-1}), Cu (7.4 ± 5.0 to 17.5 ± 15.8 g cm^2 yr^{-1}), Zn (47.2 ± 29.8 to 128.1 ± 106.9 g cm^2 yr^{-1}) and Pb (6.7 ± 4.8 to 17.8 ± 14.7 g cm^2 yr^{-1}) all increased significantly ($p < 0.01$) between these periods. In *Type II* lakes, although most ratios and fluxes showed similar increasing trends, only LOI increased significantly from 1.0 ± 0.2 (1950–1979) to 1.6 ± 0.5 g cm^2 yr^{-1} (1998-present) ($p < 0.01$) (Fig. 6b).

4. Discussion

4.1. Spatial-temporal dynamics

Results revealed significant sedimentary changes since the late 1800s, linked to anthropogenic degradation. Land-cover changes impacted sediment characteristics more than climate alone (Fig. 5). Deforestation in the LMRB began in the late 1800s due to steamship industry demands and surged after the 1970s with population growth and agricultural expansion (Davis, 2020; Etter et al., 2006). This is reflected in the marked increase in MAR and the rising nutrient and OM accumulation and heavy metal fluxes since the early 1980s (Fig. 6). Albeit these anthropic stressors, no major pollutant point source pattern was detected and sediment characteristics generally varied according to lake-river connectivity, consistent with existing tropical America literature (e.g., Monteiro et al., 2024; Almeida et al., 2014). However, novel changes in sources and deposition patterns emerged post-1980s between

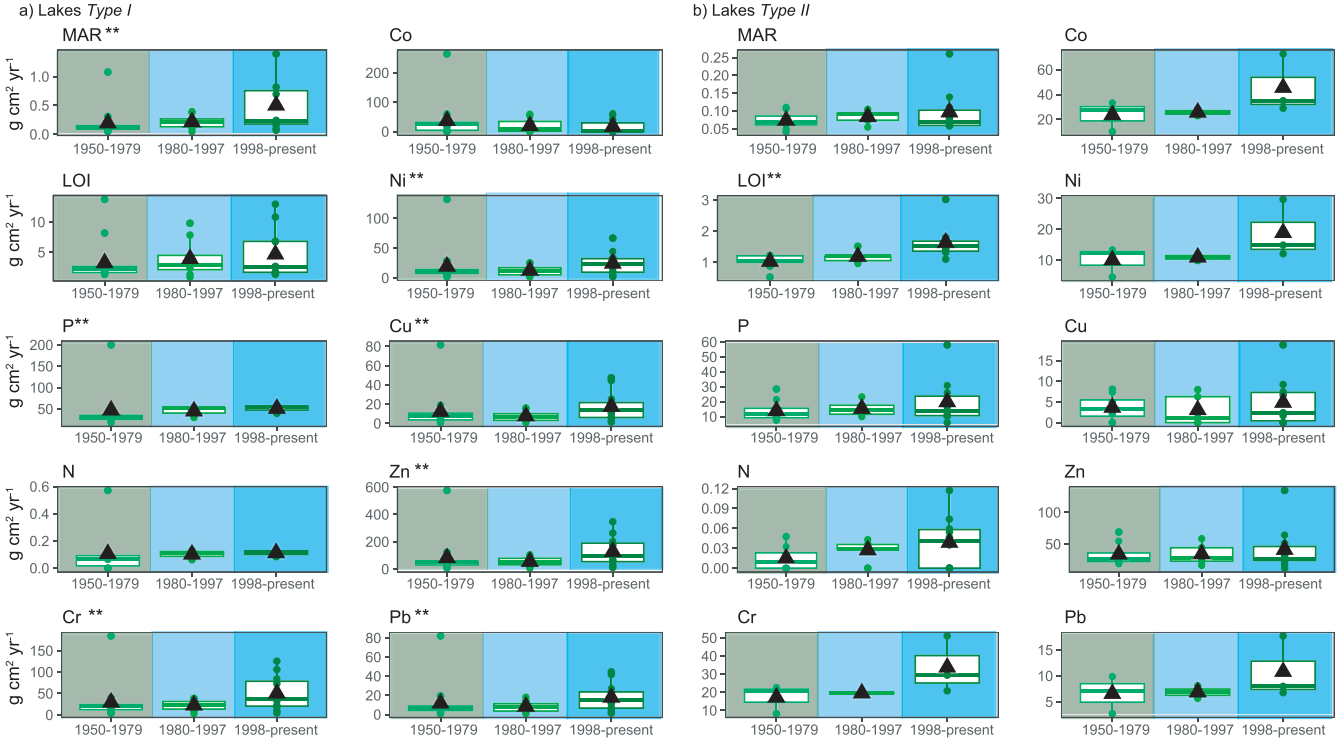

Fig. 6. Boxplots of mass accumulation rates (MAR) and elemental fluxes at lakes *Type I* (a) and *Type II* (b) during three periods of increased deforestation (1950–1979; 1980–1997; 1998-present CE). Differences between the time periods were assessed via Tukey's HDs. * $p < 0.05$; ** $p < 0.01$; *** $p < 0.001$.

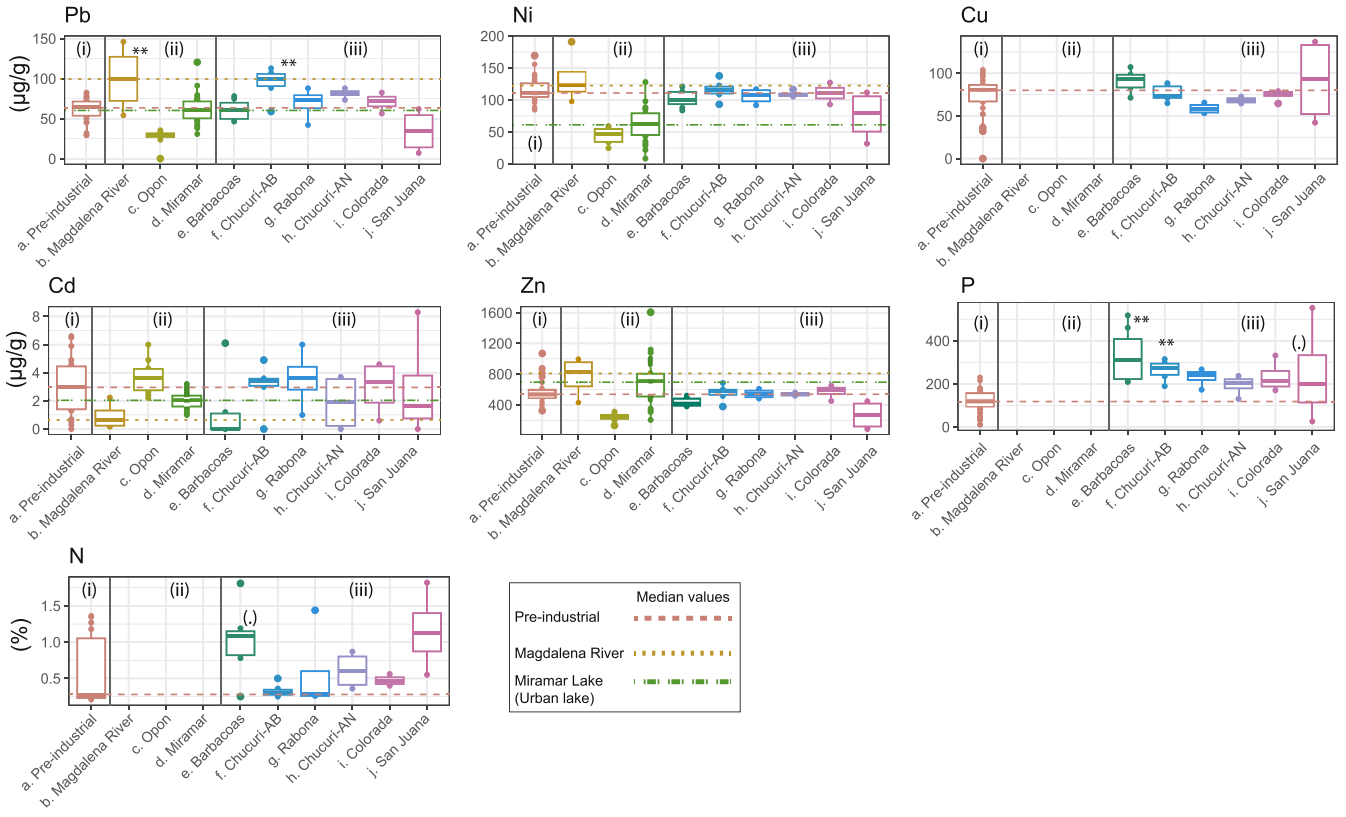

Fig. 7. Graphical representation of the historical climatic variability, land-cover change and reconstructed long-term changes in sediment biogeochemistry along lakes *Type I* and *Type II* during two detected main periods of change: pre-1980s and post 1980s CE.

connected (*Type I*) and isolated lakes (*Type II*), suggesting regional hydrological and/or climatic shifts linked to land-use changes (Fig. 7).

4.1.1. Pre-1980s

In highly connected *Type I* lakes, OM from both allochthonous (e.g., river catchment forests and wetlands) and autochthonous (e.g., phytoplankton) sources was present, as indicated by C/N ratios of 8–14 (Zhang et al., 2022; Pestana et al., 2019). These lakes, including Chucurí-AB, Rabona and Barbacoas, were enriched with Mo/Ti, V/Ti, S/Ti, and metals like Co, Zn, Ni, and Cu, suggesting reductive conditions with significant OM degradation (Zhang et al., 2022; Tribovillard et al., 2006). The joint prevalence of OM, Mo/Ti, and V/Ti enrichment in Chucurí-AB and Rabona suggest euxinic conditions, while the low Mo/Ti enrichment in Barbacoas suggests suboxic/anoxic conditions (Tribovillard et al., 2006). In contrast, isolated *Type II* lakes had higher coarse material concentrations (Zr/Fe and Ti/Ca) and lower redox conditions associated with Fe/Mn reflecting more isolated (less river input) conditions (Gaiero et al., 1997).

Type I lake sediments were linked to wetter periods, reflecting a likely greater influence of the main river's flood pulse (Pereira et al., 2024; Almeida et al., 2014). At the time, the Magdalena Basin had no major impoundments, and while deforestation rates were increasing, they remained relatively low (Etter et al., 2006). As a result, the lakes likely experienced stronger flood pulses, with the Magdalena and Carare rivers acting as conduits for large quantities of allochthonous OM, metals and nutrients, which were distinctly delivered to both lake types by the flood pulse. The larger, more connected *Type I* lakes likely had shorter water residence times allowing continuous influx of OM and finer river-derived elements to be incorporated into the lake's food web and sediments (Monteiro et al. 2024; Pestana et al., 2019; Sutfin et al., 2016). In contrast, the smaller, more isolated *Type II* lakes likely had longer residence times, which allowed detrital and coarse materials to settle over the OM. Additionally, OM in these lakes probably underwent preliminary filtration in the floodplains (Monteiro et al. 2024; Pestana et al., 2019; Sutfin et al., 2016).

4.1.2. Post-1980s

By the 1980s, sediment biogeochemistry in *Type I* lakes shifted with increased MAR, erosion (Ti/Ca), heavy metals (e.g., Pb, Cr, Cd), nutrients (P) and coarse material (Zr/Fe), while OM accumulation declined. Conversely, *Type II* lakes showed higher accumulations of nutrients (N, P) and OM and reductive conditions with reduced MAR. *Type II* sediments were enriched with V/Ti, S/Ti and metals like Co, Zn, Ni and Cu, indicating intense OM degradation and sulphide-reductive conditions. The increased P levels in *Type II* lakes suggest, however, rising anthropogenic sources rather than intensified anoxic pathways (Zhang et al., 2022).

The changes in the studied biogeochemical indicators between the *Type I* and *Type II* lakes further align with two decades of dry regional climate (Fig. 7), including the 1997–1998 El Niño event, one of the driest periods of the past six decades, which dried out much of the lakes (Lopera et al., 2021). It also coincided with surges in deforestation and the commissioning of the Betania Reservoir on the Magdalena River in 1983. This reservoir is one of the largest hydropower dams in the basin, which played a crucial role in stabilising the river's flow pulses and reducing the extent of river-lake connectivity ever since (Angarita et al., 2018).

Hydrological stabilisation from river damming and/or drier climate conditions likely reduced river-lake connectivity and increased water residence times in both lake types (Lopera-Congote et al., 2021; Salgado et al., 2020). Forest-to-agriculture land conversions in tropical America have further shown that land-cover change releases nutrients and runoff of highly labile OM, which is rapidly mineralised in rivers (Wolf et al., 2011). Since the 1980s, erosive material has steadily increased accordingly in the Magdalena River, even with dams retaining clastic material (Jiménez-Segura et al., 2022). Thus, deforestation, combined with

damming and a drier climate likely disrupted the downstream movement of OM (Sutfin et al., 2016), while boosting fluxes of erosive material and nutrients, capable of reducing OM deposition, and increased sedimentation rates in the connected *Type I* lakes (Ballogh et al., 2010). Damming and drier climates also likely increased water residence times in *Type II* lakes, leading to expanded wetland fringes, higher accumulation of nutrients and OM and faster sedimentation and anoxic conditions (Salgado et al., 2019b). The observed temporal homogenization of biogeochemical variance across all lake sediments since the 1980s (Fig. 5) also aligns with other dam-affected systems, which show regulated sedimentation patterns post-dam implementation (Zeng et al., 2018).

The higher accumulation of heavy metals in *Type I* lake sediments post-1980s also matches findings of metal pollution in human-altered

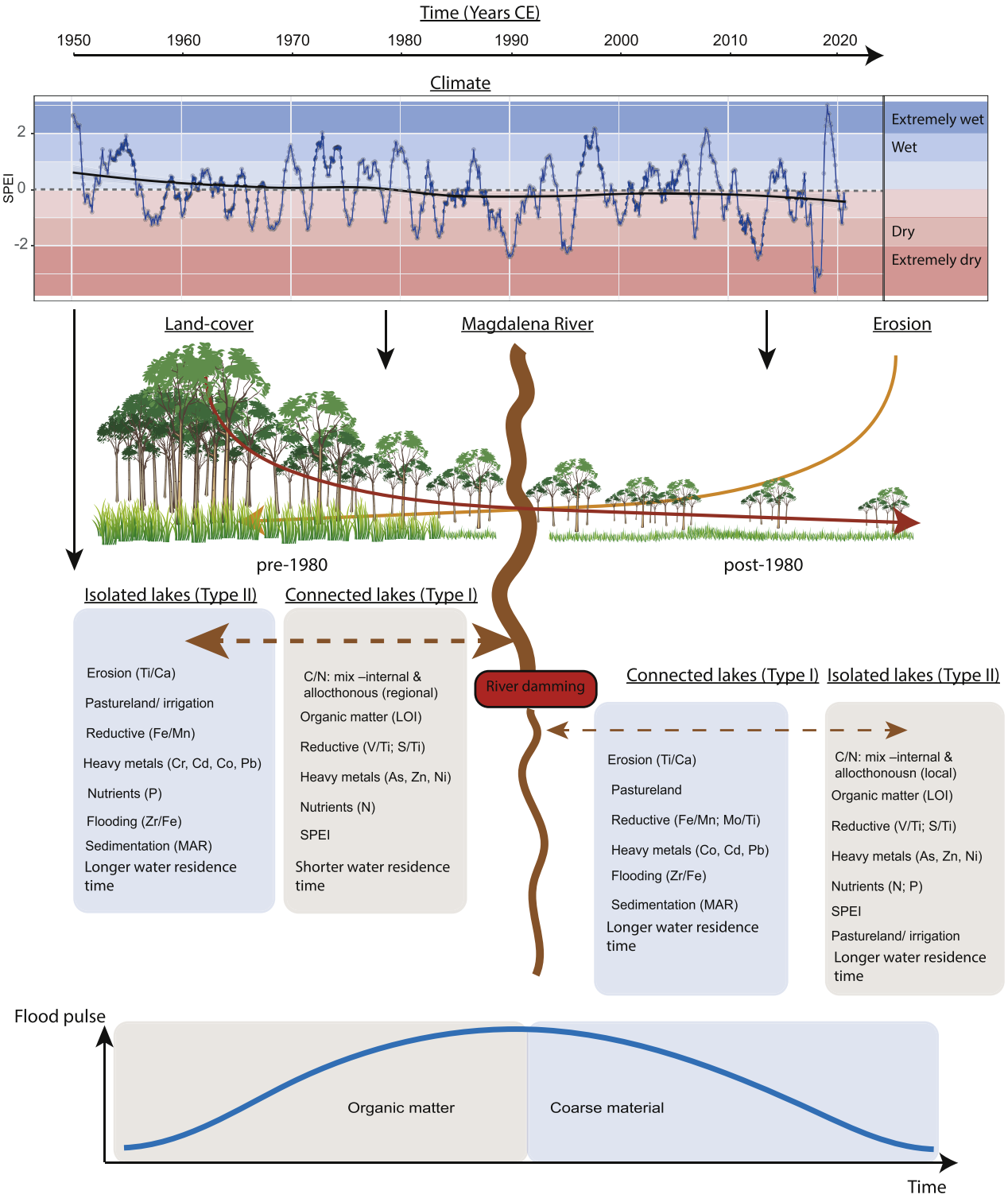

Fig. 8. Boxplots showing the variation in concentrations of elements at (i) pre-1900s (this study), (ii) in the Middle reaches of the Magdalena River (Tejeda-Benitez et al. 2016) and in the Opon and Miramar lakes (Olivero-Verbel et al., 2015b), and (iii) the study lakes surface-sediments. The significance of current concentrations exceeding the historical values were tested via Tukey Honest test. (.) $p < 0.1$; * $p < 0.05$; ** $p < 0.01$.

floodplain lakes showing elevated concentrations of these pollutants in sediments of connected, flood-prone lakes compared to isolated ones (Luo et al., 2021; Ciazela et al., 2018). Connected lakes, with larger catchment areas and flushing rates, receive more sediments and pollutants from the main river channel, while having fewer opportunities for OM to settle (Luo et al., 2021; Sutfin et al., 2016). They also often have more clay minerals from flooding, which binds metals, increasing sediment concentrations (Tack et al., 1997).

4.2. But are the lakes sediments polluted?

Enrichment factors are typically used to assess metal contamination, however the observed shifts in element sources and deposition over space and time, along with the lack of robust background levels in the Magdalena River, support the use of concentrations instead (Tribovillard et al., 2006). Accordingly, most studied element concentrations in the lakes surface-sediments remain within or below historical median levels, similar to other South American rivers like the Atrato and Amazon (Córdoba-Tovar et al., 2023; Moreno-Brush et al., 2016) (Fig. 8). However, careful consideration must be taken, as low pollutant concentrations in the sediments may be influenced by factors such as bioavailability, heavy rainfall, swift currents and increasing MAR (Palacios-Torres et al., 2018; Córdoba-Tovar et al., 2022; Pestana et al., 2019; Chen et al., 2000). Despite this potential dilution issues, since the late 1990s, there has been a clear increase in metal and nutrient accumulation, reflecting a likely increase in pollution from higher sediment fluxes from anthropogenic sources (Yang et al., 2023; Schneider et al., 2021). This trend is more pronounced in the highly connected *Type I* lakes, which are more sensitive to MAR than the isolated *Type II* lakes.

4.3. Conclusions and implications

Human-influenced tropical American riverine landscapes face widespread nutrient and heavy metal contamination (Monteiro et al., 2024; Almeida et al., 2014), with severe risks from contaminants like Hg, As, Pb and Cd (Palacios-Torres et al., 2018). Our time series analysis uncovers previously overlooked complexities, in the temporal and spatial patterns of sources and deposition, driven by land-cover changes, climatic variability and the hydrological context of the lakes. Our main supporting findings are that:

- Land cover alterations, river regulation and climatic variability have significantly and cumulatively affected lake sediment biogeochemistry, gradually (since the late 1800s).
- Since the late 1990s, nutrient, OM and heavy metal fluxes have significantly deviated from historical levels, likely reflecting increasing combined human pressures.
- Land-cover changes have a greater impact on lake sediment biogeochemistry compared to climate alone, highlighting the need to preserve forests and maintain hydrological connectivity dynamics. Indeed, protecting individual lakes is insufficient for addressing catchment-wide pollution.
- Lake connectivity to a main river influence how lakes respond to human impacts over time. Highly connected lakes receive greater fluxes of heavy metals and coarse material from flooding, while isolated lakes with longer water residence times, due to damming, tend to promote littoral productivity and anoxic conditions, thereby enhancing nutrient and OM sedimentation.
- Sources and deposition rates can change significantly over time due to climate, hydrological and/or catchment modifications, bringing complexity to establish reference conditions. Understanding these dynamics is crucial for accurate pollution assessments and effective management strategies.

AI statement

During the preparation of this work the authors used ChatGTP to check grammar, structure, and spelling. After using this tool, the authors reviewed and edited the content as needed and take full responsibility for the content of the publication.

CRediT authorship contribution statement

Jorge Salgado: Writing – review & editing, Writing – original draft, Visualization, Project administration, Methodology, Investigation, Funding acquisition, Formal analysis, Data curation, Conceptualization. **Camila Jaramillo-Monroy:** Writing – review & editing, Resources, Project administration, Funding acquisition, Data curation. **Andrés Link:** Writing – review & editing, Resources, Funding acquisition. **Laura Lopera-Congote:** Writing – review & editing, Methodology, Data curation. **Maria I. Velez:** Writing – review & editing, Resources, Funding acquisition. **Catalina Gonzalez-Arango:** Writing – review & editing, Resources, Funding acquisition. **Handong Yang:** Writing – review & editing, Methodology, Data curation. **Virginia N. Panizzo:** Writing – review & editing, Resources, Funding acquisition. **Suzanne McGowan:** Writing – review & editing, Resources, Funding acquisition.

Declaration of competing interest

The authors declare that they have no known competing financial interests or personal relationships that could have appeared to influence the work reported in this paper.

Acknowledgements

We would like to acknowledge financial support from Universidad Católica de Colombia for funding J.S and C.J through the internal research project grant (No: 000000000000637). We also thank Fundación Proyecto Primates, A. Montoya, and A. Salgado for logistic support on fieldwork, hospitality, and providing accessibility to the study area. We thank J. Shurin and N. Rose for their thoughtful comments on the initial draft, T. Needham for help with XRF analysis, and J. Lacey for C/N analysis. The collection of sediment material was assessed under the Permiso Marco de Recolección de Especímenes Silvestres de La Biodiversidad Biológica con fines de Investigación Científica No Comercial No. 1177 del 09 de octubre de 2014-IBD 0359 and the Collection Project PR.6.2015.2607 from the Facultad de Ciencias, at Universidad de los Andes.

Supplementary materials

Supplementary material associated with this article can be found, in the online version, at doi:10.1016/j.watres.2024.122633.

Data availability

Data will be made available on request.

References

Almeida, R.D., Bernardi, J.V.E., Oliveira, R.C., Carvalho, D.P.D., Manzatto, A.G., Lacerda, L.D.D., Bastos, W.R., 2014. Flood pulse and spatial dynamics of mercury in sediments in Puruzinho lake, Brazilian Amazon. Acta Amazon 44, 99–105.

Angarita, H., Wickel, A.J., Sieber, J., Chavarro, J., Maldonado-Ocampo, J.A., Delgado, J., Purkey, D., 2018. Basin-scale impacts of hydropower development on the Mompós Depression wetlands, Colombia. Hydrol. Earth Syst. Sci. 22 (5), 2839–2865.

Appleby, P.G., 2001. Chronostratigraphic techniques in recent sediments. In: Tracking Environmental Change Using Lake Sediments: Basin Analysis, Coring, and Chronological Techniques, pp. 171–203.

Balogh, S.J., Triplett, L.D., Engstrom, D.R., Nollet, Y.H., 2010. Historical trace metal loading to a large river recorded in the sediments of Lake St. Croix, USA. J. Paleolimnol. 44, 517–530.

Chen, C.Y., Stemberger, R.S., Klaue, B., Blum, J.D., Pickhardt, P.C., Folt, C.L., 2000. Accumulation of heavy metals in food web components across a gradient of lakes. Limnol. Oceanogr. 45, 152–1536.
Ciazela, J., Siepak, M., Wojtowicz, P., 2018. Tracking heavy metal contamination in a complex river-oxbow lake system: middle Odra Valley, Germany/Poland. Sci. Total Environ. 616, 9961006.
Ciszewski, D., Grygar, T.M., 2016. A review of flood-related storage and remobilization of heavy metal pollutants in river systems. Water, Air, Soil Pollut. 227, 1–19.
Córdoba-Tovar, L., Marrugo-Negrete, J., Barón, P.A.R., Díez, S., 2023. Ecological and human health risk from exposure to contaminated sediments in a tropical river impacted by gold mining in Colombia. Environ. Res. 236, 116759.
Córdoba-Tovar, L., Marrugo-Negrete, J., Barón, P.R., Díez, S., 2022. Drivers of biomagnification of Hg, As and Se in aquatic food webs: a review. Environ. Res. 204, 112226.
Davis, W., 2020. Magdalena: River of Dreams. Random House.
Davies, S.J., Lamb, H.F., Roberts, S.J., 2015. Micro-XRF core scanning in palaeolimnology: recent developments. In: Croudace, I., Rothwell, R. (Eds.), Micro-XRF Studies of Sediment Cores. Springer.
Dean, W.E., 1974. Determination of carbonate and organic matter in calcareous sediments and sedimentary rocks by loss on ignition; comparison with other methods. J. Sediment. Res. 44, 242248.
Etter, A., McAlpine, C., Pullar, D., Possingham, H., 2006. Modelling the conversion of Colombian lowland ecosystems. J. Environ. Manage. 79 (1), 74–87.
Gaiero, D.M., Ross, G.R., Depetris, P.J., Kempe, S., 1997. Spatial and temporal variability of total non-residual heavy metals content in stream sediments from the Suquia River system, Cordoba, Argentina. Water, Air, Soil Pollut. 93, 303–319.
Jiménez-Segura, L., Restrepo-Ángel, J.D., Hernandez-Serna, A., 2022. Drivers for the artisanal fisheries production in the Magdalena River. Front. Environ. sci. 1619.
Junk, W.J., Bayley, P.B., Sparks, R.E., 1989. The flood pulse concept in river-floodplain systems. Can. Spec. Publ. Fish. Aquatic Sci. 106, 110–127.
Klein Goldewijk, K., Beusen, A., Doelman, J., Stehfest, E., 2017. Anthropogenic land use estimates for the Holocene–HYDE 3.2. Earth Syst. Sci. Data 9, 927953.
Le, S., Josse, J., Husson, F., 2008. FactoMineR: an R package for multivariate analysis. J. Stat. Softw. 25, 1–18.
Lopera-Congote, L., Salgado, J., Vélez, M.I., Link, A., González-Arango, C., 2021. River connectivity and climate behind the long-term evolution of tropical American floodplain lakes. Ecol. Evol. 11, 12970–12988.
Luo, M., Yu, H., Liu, Q., Lan, W., Ye, Q., Niu, Y., Niu, Y., 2021. Effect of river-lake connectivity on heavy metal diffusion and source identification of heavy metals in the middle and lower reaches of the Yangtze River. J. Hazard. Mater. 416, 125818.
Monteiro, L.C., Vieira, L.C.G., Bernardi, J.V.E., Bastos, W.R., de Souza, J.P.R., do Nascimento Recktenvald, M.C.N., de Souza, J.R., 2024. Local and landscape factors influencing mercury distribution in water, bottom sediment, and biota from lakes of the Araguaia River floodplain, Central Brazil. Sci. Total Environ. 908, 168336.
Moreno-Brush, M., Rydberg, J., Gamboa, N., Storch, I., Biester, H., 2016. Is mercury from small-scale gold mining prevalent in the southeastern Peruvian Amazon? Environ. Pollut. 218, 150–159.
Moreno, L.F., García, L.C., Márquez, G., 1987. Productividad e importancia del bosque ripario del complejo de ciénagas de Chucurí (departamento de de Santander, Colombia). Actu. Biol. 16, 93–102.
Munar, A.M., Mendez, N., Narvaez, G., Campo Zambrano, F., Motta-Marques, D., Lyra Fialho Brêda, J.P., Angarita, H., 2023. Modelling the climate change impacts on river discharge and inundation extent in the Magdalena River basin–Colombia. Hydrol. Sci. J. 1–15.
Myers, N., Mittermeier, R.A., Mittermeier, C.G., Da Fonseca, G.A., Kent, J., 2000. Biodiversity hotspots for conservation priorities. Nature 403, 853–858.
Nanson, G.C., Croke, J.C., 1992. A genetic classification of floodplains. Geomorphology 4, 459–486.
Oksanen, J., Simpson, G., Blanchet, F., Kindt, R., Legendre, P., Minchin, P., et al. 2022. vegan: community Ecology Package. R package version 2.6–2. https://CRAN.R-project.org/package=vegan.
Olivero-Verbel, J., Caballero-Gallardo, K., Turizo-Tapia, A., 2015a. Mercury in the gold mining district of San Martin de Loba, South of Bolivar (Colombia). Environ. Sci. Pollut. Res. 22, 5895–5907.
Olivero-Verbel, J., Carranza López, L., Torres Moreno, A., Cervantes Ceballos, L., Manjarres Suarez, A., Bertel Sevilla, A., 2015b. Perfil Ambiental De La Ciénaga Miramar, Barrancabermeja – Santander /– Cartagena de Indias. Editorial Universitaria, p. 208.
Pagès, J., 2002. Analyse factorielle multiple appliquée aux variables qualitatives et Aux Données Mixtes. Rev. Statist. Appliq. 4, 5–37.
Palacios-Torres, Y., Caballero-Gallardo, K., Olivero-Verbel, J., 2018. Mercury pollution by gold mining in a global biodiversity hotspot, the Choco biogeographic region, Colombia. Chemosphere 193, 421–430.
Pereira, R., Panizzo, V.N., Bischoff, J., McGowan, S., Lacey, J., Moorhouse, H., Fazry, S., 2024. Investigating the role of hydrological connectivity on the processing of organic carbon in tropical aquatic ecosystems. Front. Earth Sci. 11, 1250889.
Pedraza, G.S., Calle, G.M., Lozano, L.C.G., 1989. Aspectos hidro-limnologicos en las ciénagas de chucuri y aguas negras (Magdalena medio, Colombia) durante un ciclo anual. Acta biol. Colomb. 1, 9–22.
Pestana, I.A., Almeida, M.G., Bastos, W.R., Souza, C.M., 2019. Total Hg and methylmercury dynamics in a river-floodplain system in the Western Amazon: influence of seasonality, organic matter and physical and chemical parameters. Sci. Total Environ. 656, 388–399.
Rajib, A., Zheng, Q., Lane, C.R., Golden, H.E., Christensen, J.R., Isibor, I.I., Johnson, K., 2023. Human alterations of the global floodplains 1992–2019. Sci. Data 10 (1), 499.
Salgado, J., Shurin, J.B., Vélez, M.I., Link, A., Lopera-Congote, L., González-Arango, C., de Luna, G., 2022. Causes and consequences of recent degradation of the Magdalena River basin, Colombia. Limnol. Oceanogr. Lett. 7, 451465.
Salgado, J., Vélez, M.I., González-Arango, C., Rose, N.L., Yang, H., Huguet, C., O'Dea, A., 2020. A century of limnological evolution and interactive threats in the Panama Canal: long-term assessments from a shallow basin. Sci. Total Environ. 729, 138444.
Salgado, J., Vélez, M.I., Caceres-Torres, L.C., Villegas-Ibagon, J.A., Bernal- Gonzalez, L. C., Lopera-Congote, L., et al., 2019a. Long-term habitat degradation drives neotropical macrophyte species loss while assisting the spread of invasive plant species. Front. Ecol. Evol. 7, 140.
Salgado, J., Sayer, C.D., Brooks, S.J., Davidson, T.A., Baker, A.G., Willby, N., Okamura, B., 2019b. Connectivity and zebra mussel invasion offer short-term buffering of eutrophication impacts on floodplain lake landscape biodiversity. Divers. Distrib. 25 (8), 1334–1347.
Schillereff, D.N., Chiverrell, R.C., Macdonald, N., Hooke, J.M., 2014. Flood stratigraphies in lake sediments: a review. Earth-Sci. Rev. 135, 17–37.
Schindler, S., Sebesvari, Z., Damm, C., Euller, K., Mauerhofer, V., Schneidergruber, A., Wrbka, T., 2014. Multifunctionality of floodplain landscapes: relating management options to ecosystem services. Landsc. Ecol. 29, 229–244.
Schneider, T., Musa Bandowe, B.A., Bigalke, M., Mestrot, A., Hampel, H., Mosquera, P.V., Grosjean, M., 2021. 250-year records of mercury and trace element deposition in two lakes from Cajas National Park, SW Ecuadorian Andes. Environ. Sci. Pollut. Res. 28, 16227–16243.
Simpson, G. 2022. *gratia: graceful ggplot-based graphics and other functions for GAMs fitted using mgcv*. R package version 0.7.3. https://gavinsimpson.github.io/gratia/.
Simpson, G.L., 2007. Analogue methods in palaeoecology: using the analogue package. J. Stat. Softw. 22, 1–29.
Simpson, G.L., 2018. Modelling palaeoecological time series using generalised additive models. Front. ecol. evol. 6, 149.
Sutfin, N.A., Wohl, E.E., Dwire, K.A., 2016. Banking carbon: a review of organic carbon storage and physical factors influencing retention in floodplains and riparian ecosystems. Earth Surf. Process. Landf. 41, 38–60.
Tack, F.M.G., Verloo, M.G., Vanmechelen, L., Van Ranst, E., 1997. Baseline concentration levels of trace elements as a function of clay and organic carbon contents in soils in Flanders (Belgium). Sci. Total Environ. 201, 113–123.
Tejeda-Benitez, L., Flegal, R., Odigie, K., Olivero-Verbel, J., 2016. Pollution by metals and toxicity assessment using *Caenorhabditis elegans* in sediments from the Magdalena River, Colombia. Environ. Pollut. 212, 238–250.
Tribovillard, N., Algeo, T.J., Lyons, T., Riboulleau, A., 2006. Trace metals as paleoredox and paleoproductivity proxies: an update. Chem. Geol. 232 (1–2), 12–32.
Tockner, K., Stanford, J.A., 2002. Riverine flood plains: present state and future trends. Environ. Conserv. 29, 308–330.
Vicente-Serrano, S.M., Beguería, S., López-Moreno, J.I., 2010. A multiscalar drought index sensitive to global warming: the standardised precipitation evapotranspiration index. J. Clim. 23, 1696–1718.
Walton, R.E., Moorhouse, H.L., Roberts, L.R., Salgado, J., Ladd, C.J., Do, N.T., Henderson, A.C., 2023. Using lake sediments to assess the long-term impacts of anthropogenic activity in tropical river deltas. Anthr. Rev., 20530196231204334
Winemiller, K.O., McIntyre, P.B., Castello, L., Fluet-Chouinard, E., Giarrizzo, T., Nam, S., Sáenz, L., 2016. Balancing hydropower and biodiversity in the Amazon, Congo, and Mekong. Science 351 (6269), 128–129.
Wittmann, F., Householder, E., de Oliveira Wittmann, A., Lopes, A., Junk, W.J., Piedade, M.T., 2015. Implementation of the Ramsar Convention on South American wetlands: an update. Res. Rep. Biod. Stud. 47–58.
Wohl, E., 2021. An integrative conceptualization of floodplain storage. Rev. Geophys. 59, e2020RG000724.
Wolf, S., Eugster, W., Potvin, C., Turner, B.L., Buchmann, N., 2011. Carbon sequestration potential of tropical pasture compared with afforestation in Panama. Glob. Change Biol. 17 (9), 2763–2780.
Wood, S.N., 2017. Generalized Additive models: an Introduction With R, 2nd edition. Chapman and Hall/CRC, New York.
Yang, H., Macario-González, L., Cohuo, S., Whitmore, T.J., Salgado, J., Peréz, L., O'Dea, A., 2023. Mercury Pollution History in Tropical and Subtropical American Lakes: multiple Impacts and the Possible Relationship with Climate Change. Environ. Sci. Technol. 57, 3680–3690.
Zeng, L., McGowan, S., Cao, Y., Chen, X., 2018. Effects of dam construction and increasing pollutants on the ecohydrological evolution of a shallow freshwater lake in the Yangtze floodplain. Sci. Total Environ. 621, 219–227.
Zhang, Y., Fu, H., Liao, H., Chen, H., Liu, Z., 2022. Geochemical records of Lake Erhai (South-Western China) reveal the anthropogenically-induced intensification of hypolimnetic anoxia in monomictic lakes. Environ. Pollut. 299, 118909.